Screw-dislocation-induced plasticization of a pinned vortex lattice

Ken Sugawara
Department of Atomic Energy, Ibaraki Polytechnic College, 864-4 Suifu-cho, Mito, Ibaraki 310-0005, Japan
(Received 5 March 2001; published 16 October 2001)

The energy of vortex-lattice screw dislocations is computed numerically on the basis of the isotropic London approximation. The results of computation are applied to the collective-pinning theory proposed by Larkin and Ovchinnikov. The present modified pinning model predicts that a vortex lattice is stabilized by possessing many screw dislocations for sufficiently strong pinning. Then the spacing between slip planes nearly equals the vortex-lattice constant, where the Burgers vectors of two adjacent slip planes are in the opposite direction. Penetration of the screw dislocations induces sudden vortex-lattice plasticization, which can be observed as a discontinuous jump of the critical current. This prediction is compared with the critical-current abrupt rises observed in amorphous Nb_xGe films and in neutron-irradiated V_3Si bulks.

DOI: 10.1103/PhysRevB.64.174512 PACS number(s): 74.60.Ge, 74.60.Jg, 74.70.Ad

I. INTRODUCTION

Although a critical-current peak effect in type-II superconductors is empirically believed to result from plasticization of a pinned vortex lattice (VL), hardly anything reliable is well known. Nearly for one decade, a further understanding of the VL plasticization has been progressing by theoretical work,[1] and this work suggests that the peak effect is relevant to a plastic vortex flow due to nucleation and motion of edge dislocations. In such theoretical work, however, the role of VL *screw* dislocations was not considered. On the other hand, Gammel *et al.*[2] have recently observed the neutron-diffraction pattern of a VL in the peak-effect regime of an Nb bulk. According to them, the longitudinal correlation length of the VL had the maximum at the onset point of the peak effect, but the transverse correlation length was not sensitive to the magnetic field. This indicates that bending deformation rather than shear deformation is essential for the peak effect.

Importance of VL screw dislocations was pointed out first by Wördenweber and Kes,[3] and by Brandt.[4–6] Wördenweber and Kes have measured the critical-current density j_c in amorphous Nb_xGe films, and found a discontinuous jump of j_c near the upper critical field. In these samples, before the jump, j_c showed a size effect (film-thickness dependence), and was excellently described by the collective-pinning theory that Larkin and Ovchinnikov[7] (LO) proposed. Magnetic fields exceeding the jump point resulted in disappearance of the size effect. This should be considered to be a crossover from two-dimensional (2-D) pinning to three-dimensional (3-D) pinning, i.e., from straight-vortex-line pinning to bending-vortex-line pinning. However, j_c after the jump deviated from the estimate based upon the 3-D version of the LO theory. Wördenweber and Kes, and also Brandt, proposed that this disparity is attributed to penetration of screw dislocations into the VL. According to them, VL's might always possess screw dislocations for 3-D pinning. For such a case, the LO theory turns invalid because of premising defect-free VL's.

Mullock and Evetts[8] (ME) have modified the LO theory, taking account of VL dislocations. Their model was based upon the concept that the correlation length corresponds to the mean distance between dislocation lines, and this model successfully described some peak effects observed in amorphous films; the peak effects can be explained in terms of VL edge dislocations.[9] However, their modification could not yet avoid the disparity concerning the j_c jump in the Nb_xGe films.[3]

In a preceding paper,[10] I have proposed that the ME model can be improved by taking account of the nonlocal effect in the VL tilt modulus. Considering this effect, I calculated the energy of VL screw dislocations within a framework of elastic-continuum theory, and estimated the energy to reduce by a factor of the Ginzburg-Landau (GL) parameter κ. Application of this estimation to the ME model led to the prediction of a discontinuous jump of j_c due to screw dislocations penetrating into a VL, and this prediction almost agrees with the observations in the Nb_xGe films.

In spite of that advantage, validity of that model should be considered dubious for the following two reasons. First, the energy estimation for VL screw dislocations is too rough. The basis of the estimation, i.e., the elastic-continuum approximation, is not valid when the spacing between VL slip planes is comparable to the vortex-lattice constant a_0; such a short spacing is predicted by the model.[10] Second, the pinning potential energy in the model was probably overestimated. As pointed out by some workers,[11] the pinning potential energy can no longer be approximated to a function linear in vortex-line displacements exceeding $a_0/2$. This point was optimistically ignored in the model. Thus, it is necessary to calculate the energy of VL screw dislocations more precisely, and necessary to reconsider collective pinning of a VL with screw dislocations more carefully. Probably such examination provides a clue to a more general problem on peak-effect mechanisms.

The present paper reports the numerical-computation results on the energy of VL screw dislocations (Sec. II), where the distance between adjacent slip planes is comparable to a_0 with their Burgers vectors being *antiparallel*. The computation is based upon the isotropic London approximation, and therefore the results are precise enough for isotropic large-κ superconductors under low magnetic fields. The computed energy is minimized when the slip-plane spacing nearly equals a_0. For this case, the computation results give practi-

cal expressions to the energy. The values of these expressions are comparable to the estimates based upon the elastic-continuum approximation, but less than these estimates. Applying the expressions to collective-pinning theory leads to the prediction that a VL stably possesses many screw dislocations for sufficiently strong pinning (Sec. III), where the present modified model allows us to premise linearity of the pinning potential energy in the vortex-line displacement. In both a superconducting film and bulk, penetration of the screw dislocations induces sudden VL plasticization accompanying a *discontinuous jump* of j_c. This prediction is compared with the critical-current abrupt rises (some kinds of peak effects) observed in amorphous Nb_xGe films[3] and in neutron-irradiated V_3Si bulks[12] (Sec. IV). The prediction for the film-pinning case is very similar to the observations in Nb_xGe. In contrast, the prediction for the bulk-pinning case is a little different from the observations in V_3Si. From this difference, I suggest that a *weakly* pinned VL in a bulk always possesses screw dislocations with the slip-plane spacing much longer than a_0.

II. ENERGY COMPUTATION FOR SCREW DISLOCATIONS

This section first presents a description of the numerical-computation procedure for the line energy density of a VL screw dislocation. The computation reveals dependence of the line energy density on the vortex-line bending rate and the applied magnetic field, where the slip-plane spacing D_c is fixed at the minimum. The bending rate is determined so that the line energy density is minimized. Next, dependence of the minimized line energy density on the slip-plane spacing is derived. As a result, we can find that the state for $D_c \simeq a_0$ can be metastable at least. Approximate expressions for the line energy density are provided for application to collective-pinning theory. Lastly, the computation results are compared with the estimates based upon the elastic-continuum approximation.

A. Procedure for computation

In an isotropic large-κ superconductor with London penetration depth λ, the total energy of vortices for a low applied magnetic field can be expressed as the sum of their self-energies and the interaction energies between them:[13]

$$E = E_{\rm self} + E_{\rm int} \tag{1}$$

with

$$E_{\rm self} = \frac{\phi_0^2}{4\pi\mu_0\lambda^2}(\ln\kappa + \alpha_{\rm core})\sum_m \int d\mathbf{r}_m$$

and

$$E_{\rm int} = \frac{\phi_0^2}{4\pi\mu_0\lambda^2}\cdot\frac{1}{2}\sum_{m\neq n}\int d\mathbf{r}_m\cdot d\mathbf{r}_n \frac{1}{|\mathbf{r}_m-\mathbf{r}_n|} \times \exp\left(-\frac{|\mathbf{r}_m-\mathbf{r}_n|}{\lambda}\right),$$

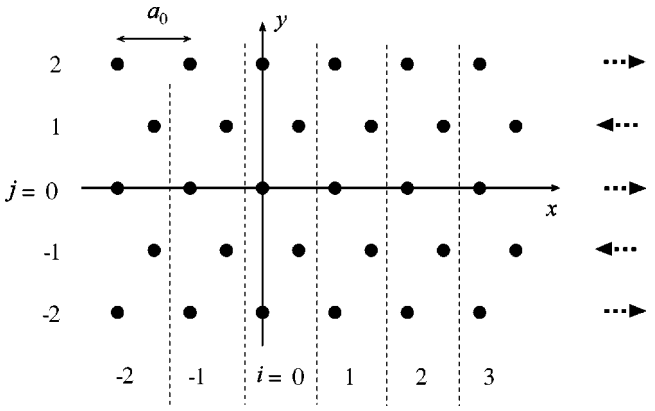

FIG. 1. A vortex lattice and a coordinate system. The solid circles denote vortex cores. The arrows indicate the directions of vortex-line displacement with the slip-plane spacing D_c equal to $\sqrt{3}a_0/2$.

where ϕ_0 is the magnetic-flux quantum, $\alpha_{\rm core}$ is the numerical constant resulting from vortex-core energy ($\simeq 0.5$), and $\mathbf{r}_m$ is the position of the mth vortex line. For the perfect vortex lattice shown in Fig. 1, the x and y components of $\mathbf{r}_m$ are given by

$$x_m = x_{i,j} = a_0\left(\frac{1-(-1)^j}{4} + i\right) \tag{2}$$

and

$$y_m = y_{i,j} = \frac{\sqrt{3}}{2}a_0 j. \tag{3}$$

When the vortex lines are bending, x_m and y_m vary as functions of the height $z_m (= z_{i,j})$.

Suppose that VL-screw-dislocation lines parallel to the x axis are spaced D_c apart in the y direction. The Burgers vectors of two adjacent dislocation lines are in the opposite direction. Let the vortex-line displacement be

$$\Delta x_{i,j}(z_{i,j}) = \begin{cases} s_{i,j}\dfrac{a_0}{4}\exp\gamma z_{i,j} & \text{for } z_{i,j} < 0 \\ s_{i,j}\dfrac{a_0}{4}[2-\exp(-\gamma z_{i,j})] & \text{for } z_{i,j} \geqslant 0 \end{cases} \tag{4}$$

with

$$s_{i,j} = \mathrm{sgn}\left\{\sin\left[\frac{\pi}{D_c}\left(y_{i,j} + \frac{\sqrt{3}}{4}a_0\right)\right]\right\} \quad \left(\frac{2D_c}{\sqrt{3}a_0} = 1,2,3,\ldots\right).$$

On the basis of Eq. (1), the line energy density of a VL screw dislocation can be expanded in

$$E_{\mathrm{SD}}=\frac{\lambda}{a_0}\left(\frac{\phi_0^2}{4\pi\mu_0\lambda^2}\right)\left[(\ln\kappa)\,{}^{\mathrm{self}}f(\gamma\lambda,a_0/\lambda)+\frac{1}{2}\sum_{j=-\infty}^{\infty}{}^{\mathrm{int}}f_j(\gamma\lambda,a_0/\lambda)\right] \tag{5}$$

with

$${}^{\mathrm{self}}f=\int_{-\infty}^{\infty}dZ_{0,0}\left[\sqrt{1+\left(\frac{dU_{0,0}}{dZ_{0,0}}\right)^2}-1\right] \tag{6}$$

and

$${}^{\mathrm{int}}f_j=\int_{-\infty}^{\infty}dZ_{0,0}\sum_{i=-\infty}^{\infty}\int_{-\infty}^{\infty}dZ_{i,j}\left[\frac{\exp(-R_{i,j})}{R_{i,j}}\times\left(1+\frac{dU_{0,0}}{dZ_{0,0}}\frac{dU_{i,j}}{dZ_{i,j}}\right)-\frac{\exp(-{}^0R_{i,j})}{{}^0R_{i,j}}\right]\quad(i^2+j^2\neq 0). \tag{7}$$

Here the following definitions are used:

$${}^0R_{i,j}=\frac{1}{\lambda}\sqrt{x_{i,j}^2+y_{i,j}^2+(z_{i,j}-z_{0,0})^2},$$

$$R_{i,j}=\frac{1}{\lambda}\sqrt{(x_{i,j}+\Delta x_{i,j}-\Delta x_{0,0})^2+y_{i,j}^2+(z_{i,j}-z_{0,0})^2},$$

$$Z_{i,j}=\frac{z_{i,j}}{\lambda},$$

and

$$U_{i,j}=\frac{\Delta x_{i,j}}{\lambda}.$$

In Eq. (5), the vortex-core contribution α_{core} is neglected; this is valid for a κ large enough. We can determine the vortex-line bending rate γ by minimizing E_{SD}.

The integration in Eq. (6) is easily carried out, and we can obtain

$${}^{\mathrm{self}}f=\frac{a_0}{2\lambda}\left[\frac{\sqrt{(a_0\gamma/4)^2+1}-1}{a_0\gamma/4}+\frac{2}{a_0\gamma}\ln\frac{4[\sqrt{(a_0\gamma/4)^2+1}-1]}{(a_0\gamma/4)^2[\sqrt{(a_0\gamma/4)^2+1}+1]}\right]. \tag{8}$$

On the other hand, the integration and summation in Eq. (7) are too complex to carry out, and numerical computation is enough to give an approximate expression to E_{SD}. In the following subsections, the computation results are reported. Here the following replacements are taken in Eq. (7):

$$\sum_{i=-\infty}^{\infty}\rightarrow\sum_{i=-N}^{N},$$

and

$$\int dZ_{i,j}\rightarrow\sum\Delta Z_{i,j},$$

where N is the minimum integer exceeding $10\lambda/a_0$. The step size and the interval of the numerical integration are as follows:

$$\Delta Z_{i,j}=0.02,\quad -\frac{10}{\gamma\lambda}\leqslant Z_{i,j}\leqslant\frac{10}{\gamma\lambda}\ \text{ for }\ \gamma\lambda\leqslant 1,$$

and

$$\Delta Z_{i,j}=\frac{0.02}{\gamma\lambda},\quad -10\leqslant Z_{i,j}\leqslant 10\ \text{ for }\ \gamma\lambda>1.$$

First, suppose that D_c reaches the shortest limit, i.e., $\sqrt{3}a_0/2$; the computation procedure for this case is the simplest. In Fig. 1, the arrows indicate the directions of vortex-line displacements for $D_c=\sqrt{3}a_0/2$. Then, it is convenient to rearrange Eq. (7) for an odd j as follows:

$${}^{\mathrm{int}}f_j={}^{\mathrm{int}}f_j^{(+)}+{}^{\mathrm{int}}f_j^{(-)} \tag{9}$$

with

$${}^{\mathrm{int}}f_j^{(+)}=\int_{-\infty}^{\infty}dZ_{0,0}\sum_{i=-\infty}^{\infty}\int_{-\infty}^{\infty}dZ_{i,j}\left(\frac{\exp(-R_{i,j})}{R_{i,j}}-\frac{\exp(-{}^0R_{i,j})}{{}^0R_{i,j}}\right) \tag{10}$$

and

$${}^{\mathrm{int}}f_j^{(-)}=\int_{-\infty}^{\infty}dZ_{0,0}\sum_{i=-\infty}^{\infty}\int_{-\infty}^{\infty}dZ_{i,j}\frac{\exp(-R_{i,j})}{R_{i,j}}\frac{dU_{0,0}}{dZ_{0,0}}\frac{dU_{i,j}}{dZ_{i,j}}. \tag{11}$$

The function ${}^{\mathrm{int}}f_j^{(+)}$ is always positive, and diverges as γ approaches zero. In contrast, ${}^{\mathrm{int}}f_j^{(-)}$ is always negative, and converges into zero with γ. Using these functions, Eq. (5) can be transformed into

$$E_{\mathrm{SD}}=\frac{\lambda}{a_0}\left(\frac{\phi_0^2}{4\pi\mu_0\lambda^2}\right)\left[\sum_{n=0}^{M}{}^{\mathrm{int}}f_{2n+1}^{(+)}(\gamma\lambda,a_0/\lambda)+F(\gamma\lambda,a_0/\lambda)\right] \tag{12}$$

with

$$F=(\ln\kappa)\,{}^{\mathrm{self}}f+\frac{1}{2}{}^{\mathrm{int}}f_0+\sum_{n=1}^{M}{}^{\mathrm{int}}f_{2n}+\sum_{n=0}^{M}{}^{\mathrm{int}}f_{2n+1}^{(-)}, \tag{13}$$

where M is the minimum integer exceeding $20\lambda/\sqrt{3}a_0$. Note that ${}^{\mathrm{int}}f_j={}^{\mathrm{int}}f_{-j}$.

While the function $F(\gamma\lambda,a_0/\lambda)$ contributes mainly to the tilt-elastic energy, the sum of ${}^{\mathrm{int}}f_j^{(+)}$ in Eq. (12) contributes only to the shear-elastic energy. The terms ${}^{\mathrm{int}}f_j^{(+)}$ for $j\geqslant 3$

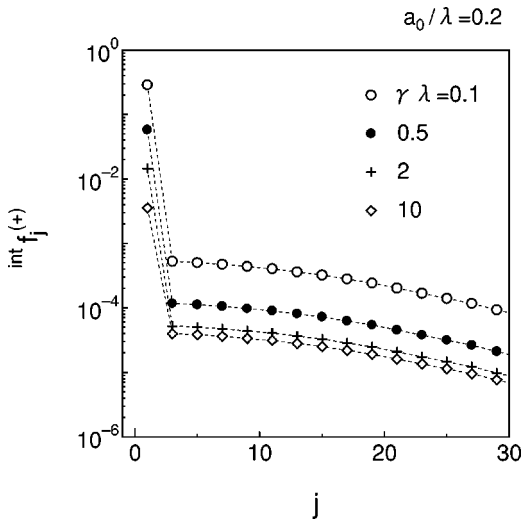

FIG. 2. Computed plots of ${}^{\rm int}f_j^{(+)}$ for $a_0/\lambda=0.2$. The dashed lines are guides for the eye. For any values of $\gamma\lambda$, the functions ${}^{\rm int}f_j^{(+)}$ for $j\geqslant 3$ are all negligible compared with ${}^{\rm int}f_1^{(+)}$.

are all negligible compared with ${}^{\rm int}f_1^{(+)}$ as demonstrated in Fig. 2, which shows computed plots of ${}^{\rm int}f_j^{(+)}$ for $a_0/\lambda=0.2$. Thus we can obtain

$$\sum_{n=0}^{M} {}^{\rm int}f_{2n+1}^{(+)} \simeq {}^{\rm int}f_1^{(+)}. \tag{14}$$

This is consistent with locality of the VL shear modulus.[13]

B. Results of computation

1. Dependence on the vortex-line bending rate

Figure 3 shows dependence of ${}^{\rm int}f_1^{(+)}$ on $\gamma\lambda$ for $a_0/\lambda=0.2$. When $\gamma\lambda\leqslant 10$, the function ${}^{\rm int}f_1^{(+)}$ can be expressed approximately by

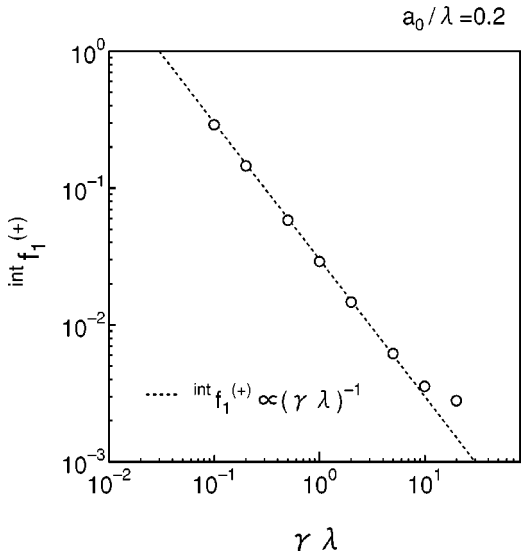

FIG. 3. Dependence of ${}^{\rm int}f_1^{(+)}$ on $\gamma\lambda$ for $a_0/\lambda=0.2$. The dashed line represents ${}^{\rm int}f_1^{(+)}=A/\gamma\lambda$ $(A=0.030)$.

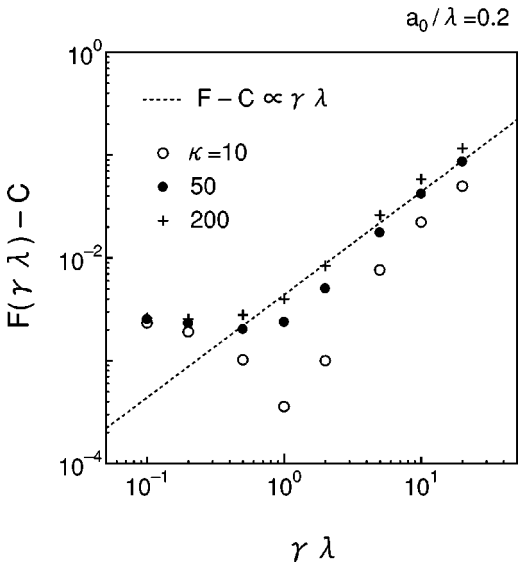

FIG. 4. Dependence of F on $\gamma\lambda$ for $a_0/\lambda=0.2$. The dashed line represents $F=B_0\gamma\lambda+C$, where the values of B_0 and C are shown in Table I.

$$ {}^{\rm int}f_1^{(+)}=\frac{A}{\gamma\lambda} \tag{15}$$

with $A=0.030$. Thus, Eq. (14) becomes

$$\sum_{n=0}^{M} {}^{\rm int}f_{2n+1}^{(+)}=\frac{A}{\gamma\lambda}. \tag{16}$$

Figure 4 shows dependence of F on $\gamma\lambda$ for $a_0/\lambda=0.2$. Near the bending rate γ such that $E_{\rm SD}$ is minimized, F is approximately linear in $\gamma\lambda$, i.e.,

$$F\simeq B_0\gamma\lambda+C \quad \text{for} \quad 0.1\ll\gamma\lambda\ll 100. \tag{17}$$

Table I shows B_0 and C obtained from fitting in Fig. 4 for several values of κ. Both parameters of $B_1\equiv B_0/\ln\kappa$ and C are almost independent of κ. Thus, reasonably, B_1 and C for $\kappa=100$ are adopted as the coefficients common to the κ range from 10 to 200.

Combining Eq. (16) and Eq. (17), we can rewrite Eq. (12) as

$$E_{\rm SD}=\frac{\lambda}{a_0}\left(\frac{\phi_0^2}{4\pi\mu_0\lambda^2}\right)\left(\frac{A}{\gamma\lambda}+B_1\gamma\lambda\ln\kappa+C\right). \tag{18}$$

TABLE I. The coefficients B_0 and C for several values of κ. The parameter a_0/λ is set to 0.2.

κ	B_0	$B_1\equiv B_0/\ln\kappa$	C
10	0.0025	0.0011	−0.0027
20	0.0033	0.0011	−0.0027
50	0.0044	0.0011	−0.0027
100	0.0053	0.0012	−0.0027
200	0.0062	0.0012	−0.0026

TABLE II. The coefficient A for several values of a_0/λ.

a_0/λ	A
0.05	0.031
0.1	0.030
0.2	0.030
0.5	0.029
1	0.027

2. Dependence on the applied magnetic field

Let us discuss magnetic-field dependence of the coefficients A, B_1, and C in Eq. (18). Table II shows A for several values of a_0/λ. The parameter A is almost independent of a_0/λ, and nearly equal to 0.030.

Figure 5 shows dependence of B_1 on a_0/λ. The dashed line represents

$$B_1 = 0.030\left(\frac{a_0}{\lambda}\right)^2, \tag{19}$$

and this equation is in good agreement with the computed plots.

Figure 6 shows variation of C versus a_0/λ. The computed plots are dispersed a little widely. This is due to large intervals by which γ varies in Fig. 4. An appropriate expression for $C(a_0/\lambda)$ is

$$C = -0.010\left[1.1\left(\frac{a_0}{\lambda}\right)^{-2/3} + 2.8\left(\frac{a_0}{\lambda}\right)^{3/2}\right]^{-1}. \tag{20}$$

The insufficient fit of the computed plots should not be considered severe, because E_{SD} is not sensitive to C.

From the results of those coefficients, Eq. (18) reduces to

$$E_{\mathrm{SD}} = \frac{\phi_0^2}{4\pi\mu_0\lambda^2}\left(\frac{0.030}{a_0\gamma} + 0.030 a_0\gamma\ln\kappa + \frac{\lambda C}{a_0}\right). \tag{21}$$

The value of the above equation is minimized when

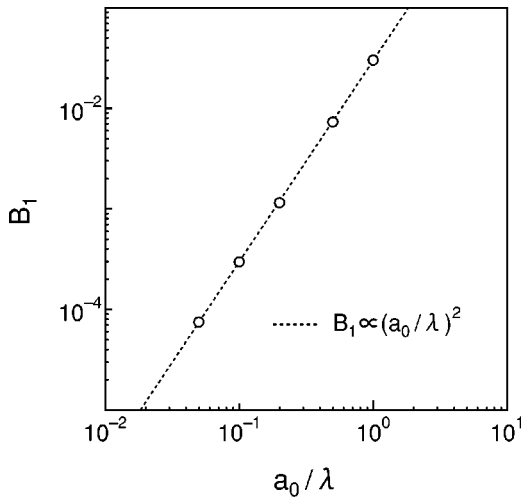

FIG. 5. Dependence of B_1 on a_0/λ. The dashed line represents $B_1 = 0.030(a_0/\lambda)^2$.

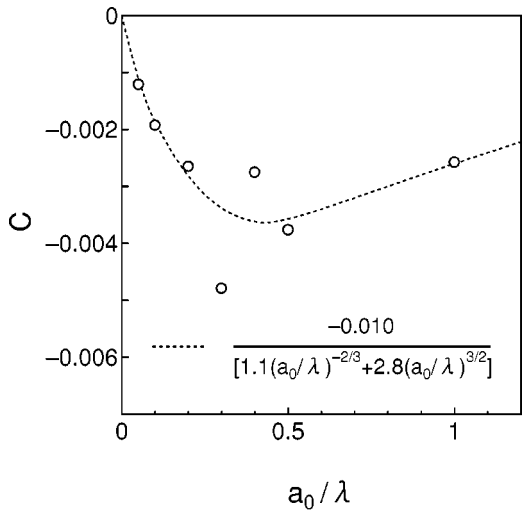

FIG. 6. Variation of C versus a_0/λ. The dashed line represents an appropriate expression for $C(a_0/\lambda)$, i.e., Eq. (20) in the text.

$$\gamma = \frac{1.0}{a_0\sqrt{\ln\kappa}}. \tag{22}$$

Then

$$E_{\mathrm{SD}} = \frac{\phi_0^2}{4\pi\mu_0\lambda^2}\left(0.060\sqrt{\ln\kappa} + \frac{\lambda C}{a_0}\right). \tag{23}$$

The first term in the parentheses dominates E_{SD}. Thus, E_{SD} is almost independent of the applied magnetic field. The above approximate expression is of an accuracy within a few percent for $\kappa \geqslant 20$, and an accuracy within about 10% for $\kappa \simeq 10$. The numerical error of the expression tends to increase with the decreasing magnetic field.

3. Dependence on the slip-plane spacing

Equation (23) is the result limited to the case of the shortest slip-plane spacing, i.e., $D_c = \sqrt{3}a_0/2$. A similar procedure enables us to compute E_{SD} for $D_c > \sqrt{3}a_0/2$.

When $D_c = \sqrt{3}a_0$, E_{SD} can be approximated to

$$E_{\mathrm{SD}} = \frac{\phi_0^2}{4\pi\mu_0\lambda^2}\left(\frac{0.030}{a_0\gamma} + (0.062\ln\kappa + 0.11)a_0\gamma + \frac{\lambda C}{a_0}\right) \tag{24}$$

with

$$C = 0.10\left(\frac{a_0}{\lambda} - 0.70\right)\left[1.0\left(\frac{a_0}{\lambda}\right)^{-4/3} + 40\left(\frac{a_0}{\lambda}\right)^{3/4}\right]^{-1}. \tag{25}$$

The value of Eq. (24) is minimized when

$$\gamma = \frac{1}{a_0\sqrt{2.1\ln\kappa + 3.7}}. \tag{26}$$

Then

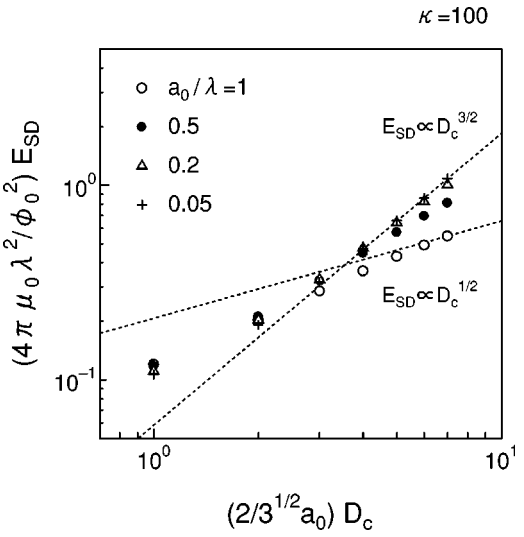

FIG. 7. Dependence of E_{SD} on D_c for $\kappa=100$. The dashed lines represent $E_{SD}\propto D_c^{3/2}$ and $E_{SD}\propto D_c^{1/2}$. When $a_0/\lambda\leqslant 0.2$, the line energy density E_{SD} is almost proportional to $D_c^{3/2}$.

$$E_{SD}=\frac{\phi_0^2}{4\pi\mu_0\lambda^2}\left(0.020\sqrt{19\ln\kappa+33}+\frac{\lambda C}{a_0}\right). \tag{27}$$

The first term in the parentheses dominates E_{SD}. Thus, E_{SD} is almost independent of the applied magnetic field. The above approximate expression is of an accuracy within a few percent for $a_0/\lambda\leqslant 0.5$, and an accuracy within about 10% for $a_0/\lambda\simeq 1$. The numerical error of the expression tends to increase with decreasing κ.

Figure 7 shows dependence of E_{SD} on D_c for $\kappa=100$. Given $E_{SD}\propto D_c^{\zeta}$, we can obtain $\zeta\simeq 3/2$ for $a_0/\lambda\ll 1$ unless $D_c\simeq a_0$; ζ approaches 1/2 with increasing a_0/λ. Thus, when $a_0\ll\lambda$, the ratio E_{SD}/D_c has a local minimum for $D_c\simeq a_0$.

Figure 8 shows variation of E_{SD}/D_c versus D_c for $\kappa a_0/\lambda=5$. When $\kappa=10$, the ratio E_{SD}/D_c has a local minimum at $D_c=\sqrt{3}a_0/2$. On the other hand, when $\kappa=100$, the ratio E_{SD}/D_c has a local minimum at $D_c=\sqrt{3}a_0$. This indicates that the state for $D_c\simeq a_0$ can be metastable at least; this point is discussed in detail in Sec. III.

C. Comparison with the elastic-continuum approximation

Let us compare the result of the above computation with that of the elastic-continuum approximation,[10] which leads to

$$E_{SD}=0.17a_0^2[c_{66}c_{44}(k=\pi/D_c)]^{1/2}\left(\frac{2D_c}{\sqrt{3}a_0}\right)^{1/2}. \tag{28}$$

Here c_{66} and $c_{44}(k)$ are the shear and tilt moduli of a VL, respectively.

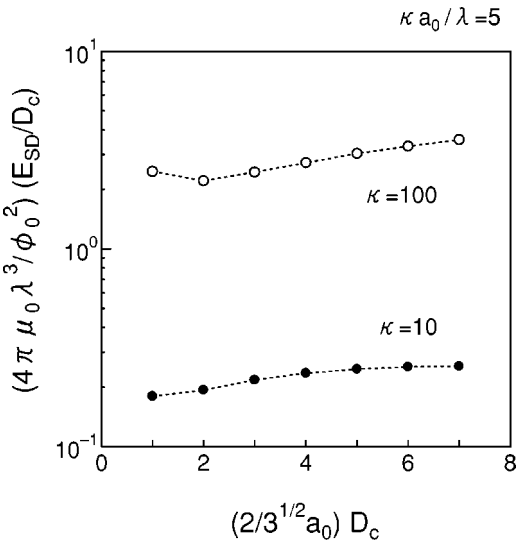

FIG. 8. Variation of E_{SD}/D_c versus D_c for $\kappa a_0/\lambda=5$. The dashed lines are guides for the eye. The ratio E_{SD}/D_c has a local minimum for $D_c\simeq a_0$. This suggests that VL's can stably possess screw dislocations of high density (i.e., $D_c\simeq a_0$).

Within a framework of the isotropic London approximation, those elastic moduli under a magnetic-flux density of B are given by[13]

$$c_{66}=\frac{H_{c2}B}{8\kappa^2} \tag{29}$$

and

$$c_{44}(k)=c_{44}^{(0)}(k)+c_{44}^{\rm corr} \tag{30}$$

with

$$c_{44}^{(0)}(k)=\frac{B^2}{\mu_0}\frac{1}{\lambda^2k^2+1}$$

and

$$c_{44}^{\rm corr}=\frac{H_{c1}B}{2\ln\kappa}\ln\left(\frac{\mu_0H_{c2}}{B}\right),$$

where H_{c1} and H_{c2} are the lower and upper critical fields, respectively. The above expressions are valid for $\mu_0H_{c1}\ll B\leqslant 0.2\mu_0H_{c2}$.

When $B\sim\mu_0H_{c2}/\kappa$, using those moduli, Eqs. (23) and (27) can be rewritten as

$$E_{SD}\simeq\begin{cases}0.14a_0^2(c_{66}c_{44}^{\rm corr})^{1/2}+E_{SD}^{(0)} & \text{for } D_c=\sqrt{3}a_0/2\,,\\ 0.21a_0^2[c_{66}c_{44}(k=4.0/a_0)]^{1/2}+E_{SD}^{(0)} & \text{for } D_c=\sqrt{3}a_0\end{cases} \tag{31}$$

with

$$E_{\mathrm{SD}}^{(0)}=\frac{\phi_0^2}{4\pi\mu_0\lambda a_0}C(<0).$$

The coefficient C is given by Eq. (20) for $D_c=\sqrt{3}a_0/2$, and by Eq. (25) for $D_c=\sqrt{3}a_0$. Although the value of Eq. (31) is less than that of Eq. (28), the two values are comparable.

In addition, the two results are similar in the dependence on D_c. From Eq. (28), it follows that

$$E_{\mathrm{SD}}\propto\begin{cases} D_c^{3/2} & \text{for } D_c\ll\lambda\ , \\ D_c^{1/2} & \text{for } D_c\gg\lambda\ . \end{cases} \tag{32}$$

The above relation is consistent with the behavior shown in Fig. 7.

III. APPLICATION TO COLLECTIVE-PINNING THEORY

In this section, the approximate expressions for E_{SD}, i.e., Eqs. (23) and (27) are applied to the collective-pinning theory proposed by Larkin and Ovchinnikov.[7] This application leads to a prediction of a discontinuous jump of the critical-current density j_c. In the first subsection, the theory for the elastic (defect-free) case[6,7,14] is outlined. In the second subsection, the theory is extended to the plastic (screw-dislocation-rich) case on the basis of the Mullock-Evetts[8] argument. In the last subsection, the extended theory describes a j_c jump, which reflects a crossover from elastic pinning to plastic pinning.

A. Pinning of a VL with no defects

When pinning centers of number density n_p exert forces f_p on vortices, the LO theory predicts that[7]

$$F_p\equiv j_cB=\left(\frac{n_p\langle f_p^2\rangle}{R_c^2L_c}\right)^{1/2}, \tag{33}$$

where R_c and L_c are the transverse and longitudinal correlation lengths, respectively; F_p is the volume pinning-force density. Unless

$$n_p\langle f_p^2\rangle\gg\frac{a_0^2}{\lambda}\left[\left(1-\frac{B}{\mu_0H_{c2}}\right)c_{66}^3c_{44}(k=0)\right]^{1/2}, \tag{34}$$

nonlocality of $c_{44}(k)$ is negligible.[6,7] Then we can roughly estimate the correlation lengths by minimizing the volume energy density of a pinned VL, i.e.,

$$U_{\text{3-D}}^{\text{elastic}}=\frac{1}{2}c_{66}\left(\frac{a_0}{2R_c}\right)^2+\frac{1}{2}c_{44}(k=0)\left(\frac{a_0}{2L_c}\right)^2-\frac{a_0}{2}\left(\frac{n_p\langle f_p^2\rangle}{R_c^2L_c}\right)^{1/2}. \tag{35}$$

Here the pinning-interaction range is set to $a_0/2$; this holds when $B\geqslant 0.2\mu_0H_{c2}$ (Refs. 4 and 15). In this way, we can obtain F_p and L_c as follows:[6,7]

$$F_p=\frac{4n_p^2\langle f_p^2\rangle^2}{a_0^3c_{66}^2c_{44}(k=0)} \tag{36}$$

and

$$L_c^{\text{elastic}}=\frac{a_0^2c_{66}c_{44}(k=0)}{2n_p\langle f_p^2\rangle}. \tag{37}$$

Then Eq. (35) becomes

$$U_{\text{3-D}}^{\text{elastic}}=-\frac{n_p^2\langle f_p^2\rangle^2}{2a_0^2c_{66}^2c_{44}(k=0)}. \tag{38}$$

In a film superconductor with thickness d shorter than L_c^{elastic}, bending of vortex lines can be neglected. In this case, the energy density is[16]

$$U_{\text{2-D}}=\frac{1}{2}c_{66}\left(\frac{a_0}{2R_c}\right)^2-\frac{a_0}{2}\left(\frac{n_p\langle f_p^2\rangle}{R_c^2d}\right)^{1/2}. \tag{39}$$

Minimizing the above equation gives

$$F_p=\left(\frac{n_p\langle f_p^2\rangle}{R_c^2d}\right)^{1/2}=\frac{2n_p\langle f_p^2\rangle}{a_0c_{66}d} \tag{40}$$

and

$$U_{\text{2-D}}=-\frac{n_p\langle f_p^2\rangle}{2c_{66}d}. \tag{41}$$

As can be seen in Eq. (40), 2-D pinning is characterized by a size effect, i.e., $j_cB=F_p\propto d^{-1}$.

B. Pinning of a VL with screw dislocations

According to Mullock and Evetts,[8] when a VL possesses screw dislocations due to pinning, the tilt-elastic-energy term in Eq. (35) should be replaced by a screw-dislocation-energy term,

$$U_{\text{3-D}}^{\text{plastic}}=\frac{1}{2}c_{66}\left(\frac{a_0}{2R_c}\right)^2+\frac{E_{\mathrm{SD}}(D_c)}{D_cL_c}-\frac{a_0}{2}\left(\frac{n_p\langle f_p^2\rangle}{R_c^2L_c}\right)^{1/2}. \tag{42}$$

The correlation length L_c corresponds to the mean longitudinal distance between screw-dislocation lines. When $L_c\gg\gamma^{-1}$, dependence of E_{SD} on L_c is negligible as can be derived from the computation result in Sec. II.

In a preceding paper,[10] I estimated the pinning-potential-energy density to be

$$-\frac{a_0}{2}\left(\frac{n_p\langle f_p^2\rangle}{R_cD_cL_c}\right)^{1/2}. \tag{43}$$

However, this is an overestimation for the vortex-line displacement expressed by Eq. (4). In a region of $z>\gamma^{-1}$, no appreciable shear deformation arises from this displacement, the result of which is equivalent to an x-directed translation of $a_0/2$ in a region of $z>\gamma^{-1}$. Thus transverse correlation

length perpendicular to screw-dislocation lines is R_c but not D_c. The above overestimation is due to premising linearity of the pinning potential energy in the vortex-line displacement. This premise is valid only for vortex-line displacements small enough; this point has recently been discussed well by some workers.[11] In fact, the pinning potential energy varies as a sinusoidal function of the VL translation with period a_0. In conclusion, estimation of the pinning-potential-energy density should be corrected as given by Eq. (42).

The volume pinning-force density F_p is determined so that Eq. (42) is minimized with respect to not only L_c and R_c but also D_c. In this equation, only the factor $E_{\rm SD}/D_c$ depends on D_c. Variation of $E_{\rm SD}/D_c$ versus D_c is shown in Fig. 8.

When $D_c \simeq a_0$, the ratio $E_{\rm SD}/D_c$ is minimized as far as we see in Fig. 8. Thus I assume here that the lowest $U_{\text{3-D}}^{\rm plastic}$ under $D_c \simeq a_0$ represents an equilibrium state. Note that too large a_0 does not allow us to assume so. For example, when $a_0/\lambda = 1$, the ratio $E_{\rm SD}/D_c$ has the maximum at $D_c \simeq a_0$.

First, let us discuss the case where $E_{\rm SD}/D_c$ is minimized for $D_c = \sqrt{3}a_0/2$; then D_c is fixed at $\sqrt{3}a_0/2$. However, when $n_p\langle f_p^2\rangle < 2c_{66}E_{\rm SD}/D_c$, the volume energy density $U_{\text{3-D}}^{\rm plastic}$ has no minimum for a finite L_c, because $\partial U_{\text{3-D}}^{\rm plastic}/\partial R_c = 0$ gives

$$U_{\text{3-D}}^{\rm plastic} = \left(\frac{E_{\rm SD}}{D_c} - \frac{n_p\langle f_p^2\rangle}{2c_{66}} \right) \frac{1}{L_c}. \tag{44}$$

In other words, the VL with screw dislocations cannot be even metastable. On the other hand, when $n_p\langle f_p^2\rangle > 2c_{66}E_{\rm SD}/D_c$, the volume energy density $U_{\text{3-D}}^{\rm plastic}$ decreases with L_c; the VL is stabilized by possessing screw dislocations of *high density* ($D_c \simeq a_0$). For $L_c \ll a_0\sqrt{\ln\kappa}$, we can approximate the vortex-line bending rate to $\gamma \sim L_c^{-1}$ instead of Eq. (22) (viz., $\gamma = 1.0/a_0\sqrt{\ln\kappa}$). Then Eq. (21) (i.e., dependence of $E_{\rm SD}$ on γ) leads to

$$E_{\rm SD} \sim \frac{\alpha_{\rm SD}}{L_c} \tag{45}$$

with

$$\alpha_{\rm SD} = \frac{\phi_0^2}{4\pi\mu_0\lambda^2}(0.030 a_0 \ln\kappa). \tag{46}$$

Thus, reasonably, $E_{\rm SD}$ in Eq. (44) is replaced by

$$E_{\rm SD} + \frac{\alpha_{\rm SD}}{L_c}, \tag{47}$$

where $E_{\rm SD}$ is defined by Eq. (23). Then minimizing $U_{\text{3-D}}^{\rm plastic}$ with respect to L_c gives

$$F_p = \frac{n_p\langle f_p^2\rangle (n_p\langle f_p^2\rangle D_c/c_{66} - 2E_{\rm SD})}{2a_0 c_{66}\alpha_{\rm SD}}, \tag{48}$$

$$L_c^{\rm plastic} = \frac{4\alpha_{\rm SD}}{n_p\langle f_p^2\rangle D_c/c_{66} - 2E_{\rm SD}}, \tag{49}$$

and

$$U_{\text{3-D}}^{\rm plastic} \simeq -\frac{D_c}{2\alpha_{\rm SD}}\left(\frac{n_p\langle f_p^2\rangle}{2c_{66}} - \frac{E_{\rm SD}}{D_c} \right)^2 \quad \text{for} \quad L_c^{\rm plastic} \gg \frac{1}{\gamma}. \tag{50}$$

For the amorphous limit ($R_c \to a_0$), Eq. (42) reduces to

$$U_{\text{3-D}}^{\rm plastic} \simeq \frac{1}{8}c_{66} + \frac{\alpha_{\rm SD}}{D_c L_c^2} - \frac{1}{2}\left(\frac{n_p\langle f_p^2\rangle}{L_c} \right)^{1/2}. \tag{51}$$

Here $R_c = a_0$ leads to $L_c \ll a_0\sqrt{\ln\kappa}$, and therefore $E_{\rm SD}$ in Eq. (42) is replaced by $\alpha_{\rm SD}/L_c$. Note that the effects of VL edge dislocations are ignored. The lowest-energy state given by Eq. (51) corresponds to Brandt's vortex-line-*spaghetti state*.[4] For this state, L_c and F_p are

$$L_c^{\rm plastic} = 4\left(\frac{\alpha_{\rm SD}^2}{n_p\langle f_p^2\rangle D_c^2} \right)^{1/3} \tag{52}$$

and

$$F_p = \frac{1}{2a_0}\left(\frac{n_p^2\langle f_p^2\rangle^2 D_c}{\alpha_{\rm SD}} \right)^{1/3}. \tag{53}$$

The above results are almost the same as those of the elastic approach.[7] The relation $L_c^{\rm elastic}/L_c^{\rm plastic} \sim (\ln\kappa)^{2/3}$ holds for the amorphous limit.

Next, let us discuss the case where $E_{\rm SD}/D_c$ is minimized for $D_c = \sqrt{3}a_0$. In this case, $E_{\rm SD}$ in Eqs. (48)–(50) is given by Eq. (27) instead of Eq. (23). Furthermore, from Eq. (24), $\alpha_{\rm SD}$ is

$$\alpha_{\rm SD} = \frac{\phi_0^2}{4\pi\mu_0\lambda^2}(0.062\ln\kappa + 0.11)a_0. \tag{54}$$

For the amorphous limit, the above equation is substituted into Eqs. (52) and (53).

When $D_c \gg a_0$, we can expect the elastic-continuum approximation to be valid; then Eq. (28) leads to the relation $E_{\rm SD}/D_c \propto D_c^{-1/2}$ for $D_c \gg \lambda$. Thus $E_{\rm SD}/D_c$ for the sufficiently long D_c is less than $E_{\rm SD}/D_c$ for $D_c \simeq a_0$. In other words, a VL with high-density screw dislocations possibly settles into merely a metastable state but not an equilibrium state (see Ref. 17). Furthermore, when $D_c \gg a_0$, we should not neglect variation of γ versus j in Eq. (4) (viz., the vortex-line displacement $\Delta x_{i,j}$). This variation causes shear deformation with a wavelength of D_c, and Eq. (43) may turn valid then. This suggests another minimum-energy state different from that represented by Eq. (50). In this state, the VL stably possesses screw dislocations of *low density* ($D_c \gg a_0$). However, I do not consider such a possibility in the present paper, because additional extensive computation is necessary for further discussion.

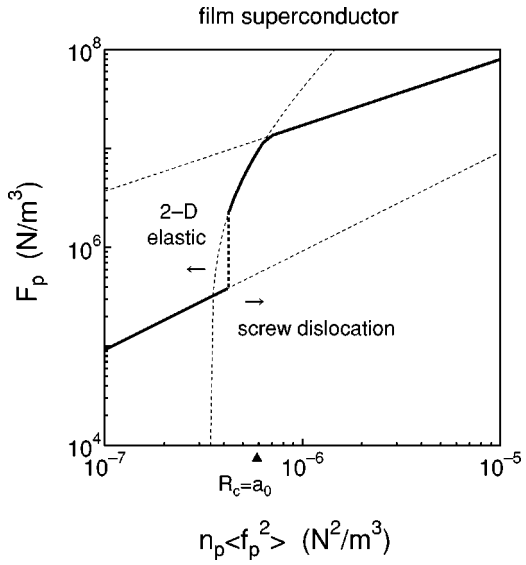

FIG. 9. A discontinuous jump of volume pinning-force density F_p in a film superconductor. The thick solid lines represent variation of F_p versus $n_p\langle f_p^2\rangle$. The thick dashed line indicates the jump. For a parameter of $n_p\langle f_p^2\rangle < 4.2\times10^{-7}$ N^2/m^3, 2-D elastic pinning occurs. Above the jump point ($n_p\langle f_p^2\rangle = 4.2\times10^{-7}$ N^2/m^3), the vortex lattice possesses high-density screw dislocations. The thin dashed lines represent Eqs. (40), (48), and (53). The triangle indicates the amorphous limit of the vortex lattice.

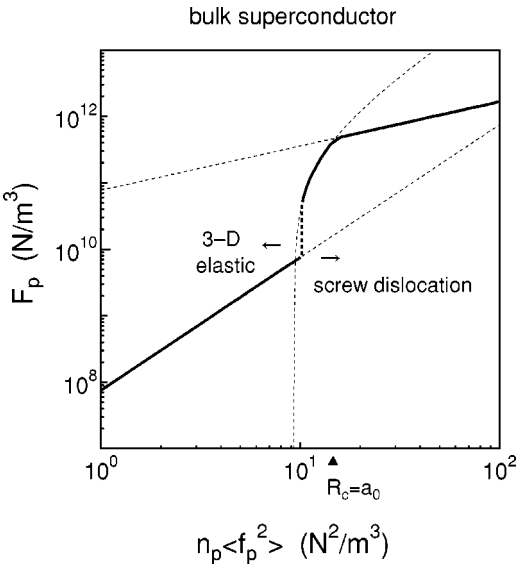

FIG. 10. A discontinuous jump of volume pinning-force density F_p in a bulk superconductor. The thick solid lines represent variation of F_p versus $n_p\langle f_p^2\rangle$. The thick dashed line indicates the jump. For a parameter of $n_p\langle f_p^2\rangle < 10$ N^2/m^3, 3-D elastic pinning occurs. Above the jump point ($n_p\langle f_p^2\rangle = 10$ N^2/m^3), the vortex lattice possesses high-density screw dislocations. The thin dashed lines represent Eqs. (36), (48), and (53). The triangle indicates the amorphous limit of the vortex lattice.

C. Screw-dislocation-induced plasticization of a pinned VL

Comparing the volume energy densities for the various pinning regimes described above, we can predict a crossover from elastic pinning to plastic pinning. For specific discussion, let us estimate $F_p \equiv j_c B$ for two different hypothetical materials, i.e., a film and a bulk superconductor.

Figure 9 shows variation of F_p versus $n_p\langle f_p^2\rangle$ in a film superconductor ($\mu_0 H_{c2}=1$ T, $\kappa=100$) with a thickness of $d=10$ μm. Here the reduced magnetic-flux density $b \equiv B/\mu_0 H_{c2}$ is set to 0.2; this corresponds to $\kappa a_0/\lambda \simeq 5$. Thus $E_{\rm SD}/D_c$ has the minimum at $D_c=\sqrt{3}a_0$, as can be seen in Fig. 8. When $n_p\langle f_p^2\rangle < 4.2\times10^{-7}$ N^2/m^3, the volume energy density $U_{2\text{-D}}$ is lower than both $U_{3\text{-D}}^{\rm elastic}$ and $U_{3\text{-D}}^{\rm plastic}$; therefore 2-D elastic pinning occurs, and F_p is given by Eq. (40). Parameters $n_p\langle f_p^2\rangle$ exceeding 4.2×10^{-7} N^2/m^3 lead to the relations $U_{3\text{-D}}^{\rm plastic} < U_{2\text{-D}} < U_{3\text{-D}}^{\rm elastic}$, and cause penetration of high-density screw dislocations into the film. The screw-dislocation lines easily move along vortex lines without Peierls forces.[3–6] Then the dislocation lines are spaced $D_c = \sqrt{3}a_0$ apart into a domain wall parallel to the film. Every time a domain wall penetrates into the film, the volume energy density stepwise decreases from $U_{2\text{-D}}$ to $U_{3\text{-D}}^{\rm plastic}$. When the mean distance between the domain walls reaches $L_c^{\rm plastic}$ given by Eq. (49), the screw dislocations no longer penetrate. Then F_p is given by Eq. (48). The relation $L_c^{\rm plastic} \ll d$ results in a discontinuous jump of $F_p \equiv j_c B$; F_p increases by a factor of about 6. At $n_p\langle f_p^2\rangle = 5.9\times10^{-7}$ N^2/m^3, the VL reaches the amorphous limit, where Eq. (53) holds. For $n_p\langle f_p^2\rangle$ in the whole range, 3-D elastic pinning never occurs stably in this film.

Figure 10 shows variation of F_p versus $n_p\langle f_p^2\rangle$ in a bulk superconductor ($\mu_0 H_{c2}=10$ T, $\kappa=10, b=0.2$) with an infinite thickness. In this case, the condition $\kappa a_0/\lambda \simeq 5$ holds. Thus $E_{\rm SD}/D_c$ has the minimum at $D_c=\sqrt{3}a_0/2$, as can be seen in Fig. 8. When $n_p\langle f_p^2\rangle < 10$ N^2/m^3, the volume energy density $U_{3\text{-D}}^{\rm elastic}$ is lower than $U_{3\text{-D}}^{\rm plastic}$; therefore 3-D elastic pinning occurs, and F_p is given by Eq. (36). Parameters $n_p\langle f_p^2\rangle$ exceeding 10 N^2/m^3 lead to the relation $U_{3\text{-D}}^{\rm plastic} < U_{3\text{-D}}^{\rm elastic}$, and cause screw-dislocation-induced plasticization of the VL. Then F_p is given by Eq. (48). The relation $L_c^{\rm plastic} \ll L_c^{\rm elastic}$ results in a discontinuous jump of $F_p \equiv j_c B$; F_p increases nearly by a factor of 7. At $n_p\langle f_p^2\rangle = 13$ N^2/m^3, the VL reaches the amorphous limit, where Eq. (53) holds. Up to this limit point, F_p steeply increases and then amounts to several tens of times of F_p before the jump. In summary, for both the film and bulk, the present modified pinning model demonstrates that $n_p\langle f_p^2\rangle$ exceeding a critical value causes a discontinuous j_c jump, which reflects sudden VL plasticization induced by screw dislocations of high density (i.e., $D_c \simeq a_0$).

IV. COMPARISON WITH EXPERIMENT

Experimental candidates for the VL plasticization predicted above are the abrupt rises of j_c in amorphous Nb_xGe films[3] and in neutron-irradiated V_3Si bulks.[12] The abrupt rises in those materials have not been explained satisfactorily by any conventional theories yet, to the best of my knowledge. In this section, the observed rises of j_c are compared with the jumps of j_c in the hypothetical materials introduced above.

A. An abrupt rise of the critical current in a film

Wördenweber and Kes[3] have found an abrupt rise of j_c near H_{c2} in amorphous Nb_xGe films, and the rise was clearly observed as a discontinuous jump. From measurement of the size effect in j_c, the jump is concluded to be due to a crossover from 2-D pinning to 3-D pinning; the size effect ($j_c \propto d^{-1}$) was observed before the jump, and disappeared after the jump. However, the jump is far different from the dimensional crossover described by the *purely* elastic approach.[3,6]

In contrast, the observed jump closely resembles the behavior predicted in Fig. 9. The film in this figure has fundamental properties similar to those of the Nb_xGe films (for example, $\mu_0 H_{c2} \simeq 4.5$ T at a temperature of 2.1 K, $\kappa = 65$, and $d = 18$ μm). The Nb_xGe film with these properties displayed a j_c jump at $b \simeq 0.8$, and j_c increased nearly by a factor of 7 then. From j_c measurement before the jump, Kes and his co-workers[3,15,16] estimated the reasonable value of $n_p\langle f_p^2\rangle/b(1-b)^2$ by using the 2-D LO theory [i.e., Eq. (40)]; $n_p\langle f_p^2\rangle/b(1-b)^2$ is independent of b, and is of order 10^{-6} N^2/m^3. On the other hand, the film in Fig. 9 displays a j_c jump at $n_p\langle f_p^2\rangle/b(1-b)^2 = 3.4\times 10^{-6}$ N^2/m^3. The two values of $n_p\langle f_p^2\rangle/b(1-b)^2$ are comparable. This agreement suggests that the observed jump was due to VL plasticization induced by high-density screw dislocations. Although such a suggestion has already been provided by Wördenweber and Kes[3] and by Brandt,[4–6] it was deficient in quantitative discussion.

A distinct difference between the observations and the present prediction is merely the following point: the j_c jump in the Nb_xGe films was observed near H_{c2}, but the j_c jump in Fig. 9 is predicted on the premise of $B \ll \mu_0 H_{c2}$, which validates the London approximation. Thus, to obtain a reliable conclusion, E_{SD} near H_{c2} should be computed on the basis of the GL theory.

In a preceding paper,[10] I proposed that the j_c jump in Nb_xGe can be explained in terms of the intermediate state between 2-D pinning and 3-D plastic pinning. However, this proposal is most likely wrong for the following reason. The prediction of the intermediate state is based upon Eq. (43), which is invalid for $D_c \sim a_0$ as described above.

B. An abrupt rise of the critical current in a bulk

Comparison for the bulk-pinning case is not successful. Meier-Hirmer *et al.*[12] have observed abrupt rises of j_c in neutron-irradiated V_3Si bulks ($\mu_0 H_{c2} \simeq 10$ T at a temperature of 10 K; $\kappa \simeq 20$). Neutron irradiation causes crystal-lattice defects, which pin the vortices. In this case, n_p corresponds to the number density of the defects, and is proportional to the neutron fluence. According to Meier-Hirmer *et al.*, the volume pinning-force density $F_p \equiv j_c B$ increased with n_p. In particular, when n_p exceeded a critical value, F_p abruptly increased by a factor of about 50. Given $F_p \propto n_p^{\zeta}$, the experiment revealed that $\zeta = 2$ below the critical n_p and $\zeta \leqslant 1$ above the critical n_p.

That behavior is in good agreement with the prediction in Fig. 10, and the bulk in this figure has fundamental properties similar to those of neutron-irradiated V_3Si bulks. From expressions for F_p, i.e., Eqs. (36) and (53), it follows that $\zeta = 2$ before the jump and $\zeta = 2/3$ at the amorphous limit.

Similar behavior, however, can be predicted also by the purely elastic approach.[12] For the bulk in Fig. 10, when $n_p\langle f_p^2\rangle$ exceeds an order of 10 N^2/m^3, nonlocality of $c_{44}(k)$ appreciably affects collective pinning; Eq. (34) holds then. Thus, F_p deviates from the local-case estimate given by Eq. (36), and exponentially increases with $n_p\langle f_p^2\rangle$ until the VL reaches the amorphous limit. This leads to an abrupt *continuous* rise of j_c. In the V_3Si bulks, indeed, the abrupt rises of j_c-versus-b curves are continuous; this appears reconcilable with the prediction for the elastic case rather than the plastic case.

Here, we should note that the predictions for both cases are different from the experimental observations in absolute values of F_p. For $b \simeq 0.2$, the experimental values of F_p near the critical n_p are two orders of magnitude smaller than the theoretical values for the bulk in Fig. 10. To begin with, as pointed out by Meier-Hirmer *et al.*,[12] F_p-versus-b curves in V_3Si deviate from the prediction by the 3-D elastic approach [i.e., Eq. (36)].

This deviation might be explained in terms of low-density VL screw dislocations, which are suggested in Sec. III. If a weakly pinned VL always possesses low-density screw dislocations stably, the VL plasticization for the bulk-pinning case falls unreal. Then, possibly, the j_c jump in V_3Si reflects an abrupt decrease in D_c, i.e., a crossover from the low-density state to the high-density state of VL screw dislocations. To confirm this suggestion, E_{SD} for a long D_c should be computed, taking account of shear deformation between slip planes.

V. CONCLUDING REMARKS

The line energy density E_{SD} of a vortex-lattice screw dislocation has been computed numerically on the basis of the isotropic London approximation, where the distance D_c between adjacent slip planes is comparable to the vortex-lattice constant a_0 with their Burgers vectors being antiparallel. When $D_c \simeq a_0$, the ratio E_{SD}/D_c is minimized. The energy density E_{SD} is approximately expressed by Eq. (23) for $D_c = \sqrt{3}a_0/2$, and by Eq. (27) for $D_c = \sqrt{3}a_0$. Both approximate expressions are almost independent of the applied magnetic field. The computed E_{SD} is comparable to the estimate based upon the elastic-continuum approximation,[10] but always less than this estimate.

Applying the computation results [i.e., Eqs. (23) and (27)] to collective-pinning theory, I have predicted the high-density state ($D_c \simeq a_0$) of vortex-lattice screw dislocations for sufficiently strong pinning. In both a superconducting film and bulk, penetration of the screw dislocations causes a discontinuous j_c jump, which reflects sudden plasticization of a pinned vortex lattice.

That prediction has been compared with experiments on amorphous Nb_xGe films[3] and neutron-irradiated V_3Si bulks.[12] Although the j_c jump in Nb_xGe has not been explained by any conventional pinning models satisfactorily, comparison between the present modified model and the ex-

periment is more successful. On the other hand, between the prediction and the observations in V_3Si, some discrepancies have been found. To avoid the discrepancies, possibly, we should introduce the low-density state ($D_c \gg a_0$) of vortex-lattice screw dislocations.

For further decent comparison with the experiments, it is necessary to compute E_{SD} for applied magnetic fields in the wider range on the basis of the GL theory, and such computation should be extended to a more general case including $D_c \gg a_0$. Probably such effort gives a step toward a complete understanding of critical-current peak effects.

ACKNOWLEDGMENTS

This work benefitted from the use of facilities in Sophia University. I would like to thank Professor Tomoyuki Sekine for critical reading of this manuscript. I would also like to acknowledge advice on numerical computation from Dr. Haruhiko Kuroe and Mrs. Yoshiko Tanokura.

[1] A. Brass, H. J. Jensen, and A. J. Berlinsky, Phys. Rev. B **39**, 102 (1989); A.-C. Shi and A. J. Berlinsky, Phys. Rev. Lett. **67**, 1926 (1991); A. E. Koshelev and V. M. Vinokur, *ibid.* **73**, 3580 (1994); A. E. Khalil, Phys. Rev. B **54**, 12 437 (1996); M.-C. Cha and H. A. Fertig, Phys. Rev. Lett. **80**, 3851 (1998); C. J. Olson, C. Reichhardt, and F. Nori, *ibid.* **81**, 3757 (1998); I. S. Aranson, S. Scheidl, and V. M. Vinokur, Phys. Rev. B **58**, 14 541 (1998); C. J. Olson and C. Reichhardt, *ibid.* **61**, R3811 (2000); Y. Cao, Z. Jiao, and H. Ying, *ibid.* **62**, 4163 (2000).

[2] P. L. Gammel, U. Yaron, A. P. Ramirez, D. J. Bishop, A. M. Chang, R. Ruel, L. N. Pfeiffer, E. Bucher, G. D'Anna, D. A. Huse, K. Mortenzen, M. R. Eskildsen, and P. H. Kes, Phys. Rev. Lett. **80**, 833 (1998).

[3] R. Wördenweber and P. H. Kes, Phys. Rev. B **34**, 494 (1986); P. H. Kes and R. Wördenweber, J. Low Temp. Phys. **67**, 1 (1987); R. Wördenweber and P. H. Kes, Cryogenics **29**, 321 (1989).

[4] E. H. Brandt, Phys. Rev. Lett. **57**, 1347 (1986).

[5] E. H. Brandt, Phys. Rev. B **34**, 6514 (1986).

[6] E. H. Brandt, J. Low Temp. Phys. **64**, 375 (1986).

[7] A. I. Larkin and Yu. N. Ovchinnikov, J. Low Temp. Phys. **34**, 409 (1979).

[8] S. J. Mullock and J. E. Evetts, J. Appl. Phys. **57**, 2588 (1985).

[9] R. Wördenweber, P. H. Wes, and C. C. Tsuei, Phys. Rev. B **33**, 3172 (1986).

[10] K. Sugawara, J. Low Temp. Phys. **117**, 127 (1999).

[11] T. Nattermann, Phys. Rev. Lett. **64**, 2454 (1990); T. Giamarchi and P. L. Doussal, Phys. Rev. B **52**, 1242 (1995).

[12] R. Meier-Hirmer, H. Küpfer, and H. Scheurer, Phys. Rev. B **31**, 183 (1985).

[13] E. H. Brandt, J. Low Temp. Phys. **26**, 735 (1977); E. H. Brandt and A. Sudbø, Physica C **180**, 426 (1991).

[14] G. Blatter, M. V. Feigel'man, V. B. Geshkenbein, A. I. Larkin, and V. M. Vinokur, Rev. Mod. Phys. **66**, 1125 (1994).

[15] R. Wördenweber, A. Pruymboom, and P. H. Kes, J. Low Temp. Phys. **70**, 253 (1988).

[16] P. H. Kes and C. C. Tsuei, Phys. Rev. Lett. **47**, 1930 (1981); Phys. Rev. B **28**, 5126 (1983).

[17] From Eq. (28), the ratio E_{SD}/D_c converges into zero as D_c diverges. In Eq. (28), however, dependence of E_{SD} on L_c is not taken into account. For the dislocation-free limit (i.e., $D_c \to \infty$), we should expect the screw-dislocation energy E_{SD}/D_cL_c to reach the tilt-elastic energy $(1/2)c_{44}(a_0/L_c)^2$. In fact, E_{SD}/D_cL_c for $D_c \simeq a_0$ becomes less than $(1/2)c_{44}(a_0/L_c)^2$ when L_c is short enough.